

1 **Assessing reliable human mobility patterns from higher-order memory in**
2 **mobile communications**

3 Joan T. Matamalas*, Manlio De Domenico*, and Alex Arenas

4 *Departament d'Enginyeria Informàtica i Matemàtiques,*
5 *Universitat Rovira i Virgili, 43007 Tarragona, Spain*

6 Understanding how people move within a geographic area, e.g. a city, a country or the
7 whole world, is fundamental in several applications, from predicting the spatio-temporal
8 evolution of an epidemics to inferring migration patterns. Mobile phone records provide an
9 excellent proxy of human mobility, showing that movements exhibit a high level of memory.
10 However, the precise role of memory in widely adopted proxies of mobility, as mobile phone
11 records, is unknown. Here we use 560 millions of call detail records from Senegal to show that
12 standard Markovian approaches, including higher-order ones, fail in capturing real mobility
13 patterns and introduce spurious movements never observed in reality. We introduce an
14 adaptive memory-driven approach to overcome such issues. At variance with Markovian
15 models, it is able to realistically model conditional waiting times, i.e. the probability to stay
16 in a specific area depending on individual's historical movements. Our results demonstrate
17 that in standard mobility models the individuals tend to diffuse faster than what observed
18 in reality, whereas the predictions of the adaptive memory approach significantly agree with
19 observations. We show that, as a consequence, the incidence and the geographic spread of
20 a disease could be inadequately estimated when standard approaches are used, with crucial
21 implications on resources deployment and policy making during an epidemic outbreak.

22 **Keywords:** Human Mobility, Markovian Model, Epidemics Spreading, Complex Networks,
23 Diffusion

24

I. INTRODUCTION

25 People move following complex dynamical patterns at different geographical scales, e.g. among
26 areas of the same city, among cities and regions of the same country or among different countries.
27 Such patterns have been recently revealed by using human mobility proxies [1–5] and, intriguingly,
28 some specific patterns tend to repeat more than others, with evidences [6, 7] of memory of mean-
29 ingful locations playing a fundamental role in our understanding of human mobility. In fact, human
30 dynamics might significantly affect how epidemics spread [2, 6, 8–10] or how people migrate from
31 one country to another [4].

32 The collaboration between researchers and mobile operators recently opened new promising di-
33 rections to gather information about human movements, country demographics and health, faster
34 and cheaper than before [1, 10–18]. In fact, mobile phones heterogeneously penetrated both rural
35 and urban communities, regardless of richness, age or gender, providing evidences that mobile
36 technologies can be used to obtain real-time information about individual’s location and social
37 activity, in order to build realistic demographics and socio-economics maps of a whole country [19].
38 Mobile data have been successfully used in a wide variety of applications, e.g., to estimate popu-
39 lation densities and their evolution at national scales [13], to confirm social theories of behavioral
40 adaptation [20] and to capture anomalous behavioral patterns associated to religious, catastrophic
41 or massive social events [21]. Even more recently, the public availability of mobile phone data sets
42 further revolutionized the field, e.g., by allowing ubiquitous sensing to map poverty, to monitor
43 social segregation and to optimize information campaigns to reduce epidemics spreading [14, 22],
44 to cite just some of them [18].

45 Although some limitations, mobile phone data still provide one the most powerful tools for
46 sensing complex social systems and represent a valuable proxy for studies where human mobility
47 plays a crucial role [1–4, 6, 8–10, 15, 22–24]. Milestone works in this direction have shown that
48 human trajectories exhibit more temporal and spatial regularity than previously thought. Individ-
49 uals tend to return to a few highly frequented locations and to follow simple reproducible patterns
50 [1, 5], allowing a higher accuracy in predicting their movements [3] and significantly affecting the
51 spreading of transmittable diseases [6]. However, the increasing interest for using mobile phone
52 data in applications should be accompanied by a wise usage of the information they carry on. In
53 fact, an inadequate model accompanied by incomplete data and scarce knowledge of other funda-
54 mental factors influencing the model itself, might lead, for instance, to a wrong estimation of the
55 incidence of an epidemics and its evolution [25].

56 Here, we used high-quality mobile phone data, consisting of more than 560 millions of call de-
 57 tail records, to show that standard approaches might significantly overestimate mobility transitions
 58 between distinct geographical areas, making difficult to build a realistic model of human mobility.
 59 To overcome this issue, we developed an adaptive memory-driven model based on empirical ob-
 60 servations that better captures existing correlations in human dynamics, showing that it is more
 61 suitable than classical memoryless or higher-order models to understand how individuals move and,
 62 for instance, might spread a disease.

63 II. MATERIALS AND METHODS

64 A. Markovian model of human mobility

65 Let us consider a physical mobility network composed by nodes, representing geographic areas,
 66 connected by weighted edges, representing the fraction of individual movements among them.
 67 Usually, the weights are inferred from geolocated activities of individuals, e.g. the consecutive
 68 airports where a plane departs and lands or, as in this work, the cell towers where a person makes
 69 consecutive calls.

70 A standard approach to deal with mobility models of dynamics [3, 4, 6, 10, 15, 16, 26] is to
 71 consider each node as a state of a Markov process, obtaining the flux between any pair of nodes from
 72 consecutive calls, and to build a mobility matrix F_{ij} encoding the probability that an individual
 73 in node i will move to node j ($i, j = 1, 2, \dots, n$). Here, we use a similar approach to build the
 74 mobility matrix for each individual $\ell = 1, 2, \dots, \mathcal{L}$ separately and we then average over the whole
 75 set of mobility matrices, to obtain the transition probability of an individual, on average:

$$F_{ij} = \frac{\sum_{\ell=1}^{\mathcal{L}} f_{ij}^{(\ell)}}{\sum_{\ell=1}^{\mathcal{L}} \sum_{k=1}^n f_{ik}^{(\ell)}}, \quad (1)$$

76 where $f_{ij}^{(\ell)}$ is the number of times the individual ℓ makes at least one call in node j after making
 77 at least one call in node i .

78 We did not impose a specific time window to calculate transitions, to avoid introducing biases
 79 and undesired effects due to the choice of the temporal range and it is worth remarking that
 80 other normalizations can be considered depending on data and metadata availability [15]. Where
 81 not otherwise specified, we considered the mobility matrix obtained from the whole period of
 82 observation. This model is known as “first-order” (or 1-memory) because the present state is the

83 only information required to choose the next state. Although very useful, this has the fundamental
 84 disadvantage that it does not account for mobility memory. In fact, it is very likely that an
 85 individual moves to a neighboring area (by means of a car or public transportation) to work and
 86 after a few hours he or she will go back to the original position. This effect has been shown to be
 87 relevant, for instance, at country level, where individuals fly from one city to another and often
 88 go back to their origin instead of moving towards a different city [7]. This memory is an intrinsic
 89 property of human mobility and must be taken into account for a realistic modeling of people
 90 movements between different geographic areas. When memory is taken into account, each physical
 91 node (e.g., $i \in \mathcal{A}$) is replaced by the corresponding state-nodes (e.g., $i \triangleleft j \in \tilde{\mathcal{A}}$ if memory is of order
 92 2) encoding the information that an individual is in node i when he or she comes from j . While
 93 \mathbf{F} encodes information about the network of n physical nodes, we need to introduce a new matrix
 94 \mathbf{H} to encode information about the network of n^2 state-nodes, accounting for the allowed binary
 95 combinations (e.g. $k \triangleleft j$, $j, k = 1, 2, \dots, n$) between physical nodes. Similarly, higher-order memory
 96 can be taken into account by building appropriate matrices.

97 We use different mobility matrices to build different mobility models. Let $N_i(t)$ indicate the
 98 population of the physical node $i \in \mathcal{A}$ at time t , then the n mobility equations describing how the
 99 flux of people diffuses through the network are given by

$$N_i(t+1) = \sum_{j=1}^n F_{ji} N_j(t). \quad (2)$$

100 In the case of τ -memory, we indicate by $\tilde{N}_\alpha(t)$ the population of the state-node $\alpha \in \tilde{\mathcal{A}}$ at time t
 101 and the n^τ mobility equations required to describe the same process are given by

$$\tilde{N}_\alpha(t+1) = \sum_{\rho=1}^{n^\tau} H_{\rho\alpha} \tilde{N}_\rho(t). \quad (3)$$

102 The population in each physical node at time t is given by the sum of the population in the
 103 corresponding state-nodes. It is worth remarking that, in general, the matrix \mathbf{H} can be a function
 104 of time as well and the equations would keep their structural form.

105 **B. Adaptive memory model of human mobility**

106 However, spatial human mobility is quite complex and (higher-order) Markovian dynamics
 107 might not be suitable to model peculiar patterns such as returning visits and conditional waiting
 108 times, i.e. the probability to stay in a location depending on the origin of the travel.

109 We will discuss better this point in the following. Let us consider, for instance, the call sequence
110 *BBBBCCCSSS* made by an individual traveling between three American cities: Chicago, Boston
111 and San Antonio. The main drawbacks of Markovian models – of order lower than three – become
112 evident in a scenario like this one, because the number of consecutive calls in the same city exceeds
113 the memory of the model and the spatial information about previously visited locations is lost.
114 Clearly, in presence of more complicated patterns, increasing the order of the model will not solve
115 the issue and some information will be inevitably lost. Alternatively, we could aggregate consecutive
116 calls in the same place to a single identifier, e.g. the previous sequence would be reduced to *BCS*.
117 In this case, a Markovian model would preserve the spatial information and correctly identify the
118 transitions between the three cities, at the price of losing information about how many calls have
119 been made in each place.

120 In absence of detailed temporal information about calling activity, the number of consecutive
121 calls in a specific location can be used as a proxy: higher the number of calls larger the waiting
122 time. The temporal information about the amount of time spent in each location is critical for
123 many dynamical processes like spreading or congestion. We assert that this time, like the next
124 visited location, is conditioned by previous movements of the individuals. To illustrate this, we
125 use the example shown in Fig. 1, where people from three different places (nodes blue, green and
126 orange) go to the same destination (node red), stay some time in there, and come back to the
127 origin of their trip. The self-loops in the central (red) node represent the time spent there, the
128 color encoding individuals coming from different origins and the size encoding the amount of time
129 spent. For instance, individuals coming from the blue node wait more than individuals coming
130 from the green node. This type of dependence is what we call conditional waiting time.

131 To better appreciate this fact, let us consider holiday trips. Individuals making expensive
132 intercontinental trips tend to spend more time visiting the destination than individuals making
133 cheaper trips, achieving a good trade-off between the travel cost and the time spent. Another
134 emblematic case is urban mobility. For instance, the red node might be an expensive commercial
135 area, the green node a wealthy neighborhood and the blue node a less wealthy area. In this scenario,
136 that should be considered only for illustrative purposes, individuals coming from the less wealthy
137 area are more likely to be qualified workers in the commercial one, with long and frequent visits.
138 Conversely, individuals from the wealthy are more likely to make unfrequent and shorter visits for
139 shopping, for instance.

140 The importance of accounting for conditional waiting times will be evident later, when we will
141 consider the spreading of an epidemics in a country.

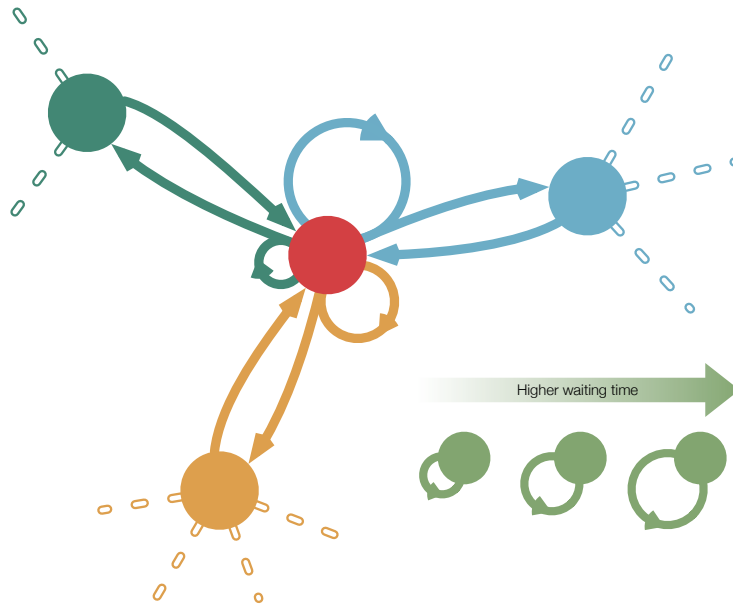


FIG. 1. **Conditional waiting times.** An example of human mobility between four different places. Individuals from green, blue and orange nodes move to the red central node and, after some time, go back to their previous location. The amount of time spent in the red node by individuals coming from the other nodes depends on their previous location, and it is represented by self-loops of different size.

142 Here, we propose a mobility model, that we name *adaptive memory*, able to account for condi-
 143 tional waiting times. At first order, the method is equivalent to a classical first-order Markovian
 144 model, whereas significant differences emerge for increasing memory with respect to standard ap-
 145 proaches. For instance, at second order, the 2-memory mobility matrix is built between all possible
 146 pairs of nodes (2-states), as in a standard second-order Markovian model. However, instead of con-
 147 sidering transitions between areas in the sequence of calls, as a second-order Markovian model does,
 148 transitions in the sequence of distinct geographical areas are considered. This point is crucial, and
 149 we better clarify it with the example shown in Fig. 2, where the differences between adaptive mem-
 150 ory and Markovian models, in terms of probability assigned to different mobility patterns, are
 151 reported.

152 The importance of such differences is reflected in the ability of each model to predict succes-
 153 sive individual movements. In fact, the presence of spurious or under-represented patterns might
 154 significantly affect the results, as shown in Fig. 3. In this example, two sequences of phone calls
 155 generated by two different users moving between three cities – B, C and S – are considered. Marko-
 156 vian models generate spurious patterns that are never observed in the data, issue not affecting the
 157 adaptive memory model by construction. Moreover, our approach predicts the next movement with

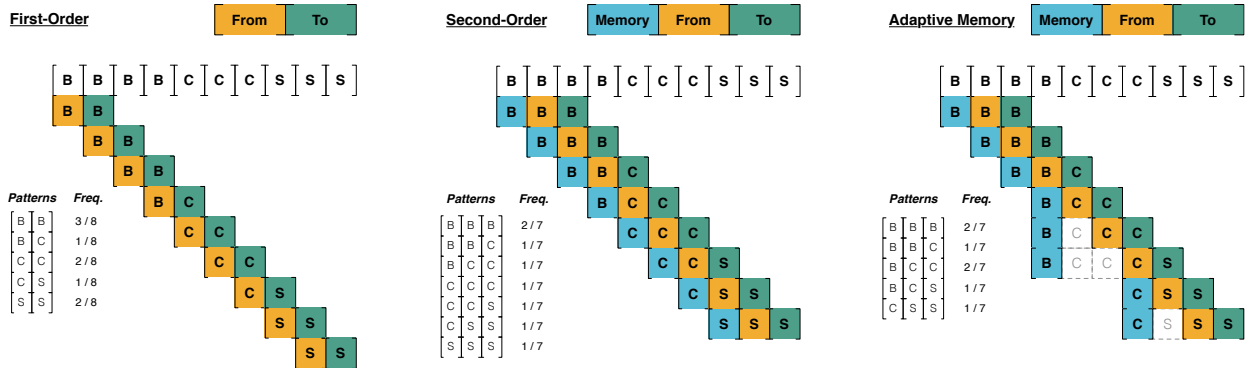


FIG. 2. **Comparing different mobility models.** Mobility models built from a representative sequence of mobile phone calls (BBBBCCSSS) made, for instance, by an individual during travels between three American cities, namely Chicago (C), San Antonio (S) and Boston (B). Let us focus on the pattern $S \leftarrow C \leftarrow B$, that is the real sequence of movements in the geographical space. The first-order model predicts a probability of $\frac{1}{64}$, the second-order model a probability of $\frac{1}{49}$, whereas the adaptive 2-memory estimates a probability of $\frac{1}{7}$, closer to observation.

158 more accuracy than Markovian ones, because it correctly takes into account conditional waiting
 159 times.

160 The difference between the adaptive memory and Markovian models becomes more evident
 161 when the corresponding transition matrices are compared. There is no difference at the first order,
 162 thus we will focus on the comparison between τ -order Markovian and adaptive τ -memory models,
 163 in the following.

164 In both models, the number of possible transitions between state nodes is the same and equals
 165 $n^{2(\tau-1)}$, where n is the number of physical nodes. For instance, in second-order models, there
 166 are $n^2 \times n^2$ transition matrices with n^3 possible transitions between state nodes, as shown in
 167 Fig. 4. However, the way how each model stores repeating calls in the same physical node is
 168 very different. While adaptive memory stores this information into the n^τ diagonal elements of
 169 the matrix, encoding the conditional waiting times discussed in the previous section, Markovian
 170 models redistribute this information among off-diagonal entries, because they do not allow this
 171 type of self-loops by construction.

172 More specifically, the information is redistributed among transitions between state nodes of the
 173 same physical node. The entries of off-diagonal blocks – corresponding to transitions between state
 174 nodes of different physical nodes – are the same in both models. Therefore, while the stationary
 175 probability of finding a random walker in a physical node is not different in the two models, it
 176 is different at the level of state nodes and, as we will see later, this significantly affects diffusion

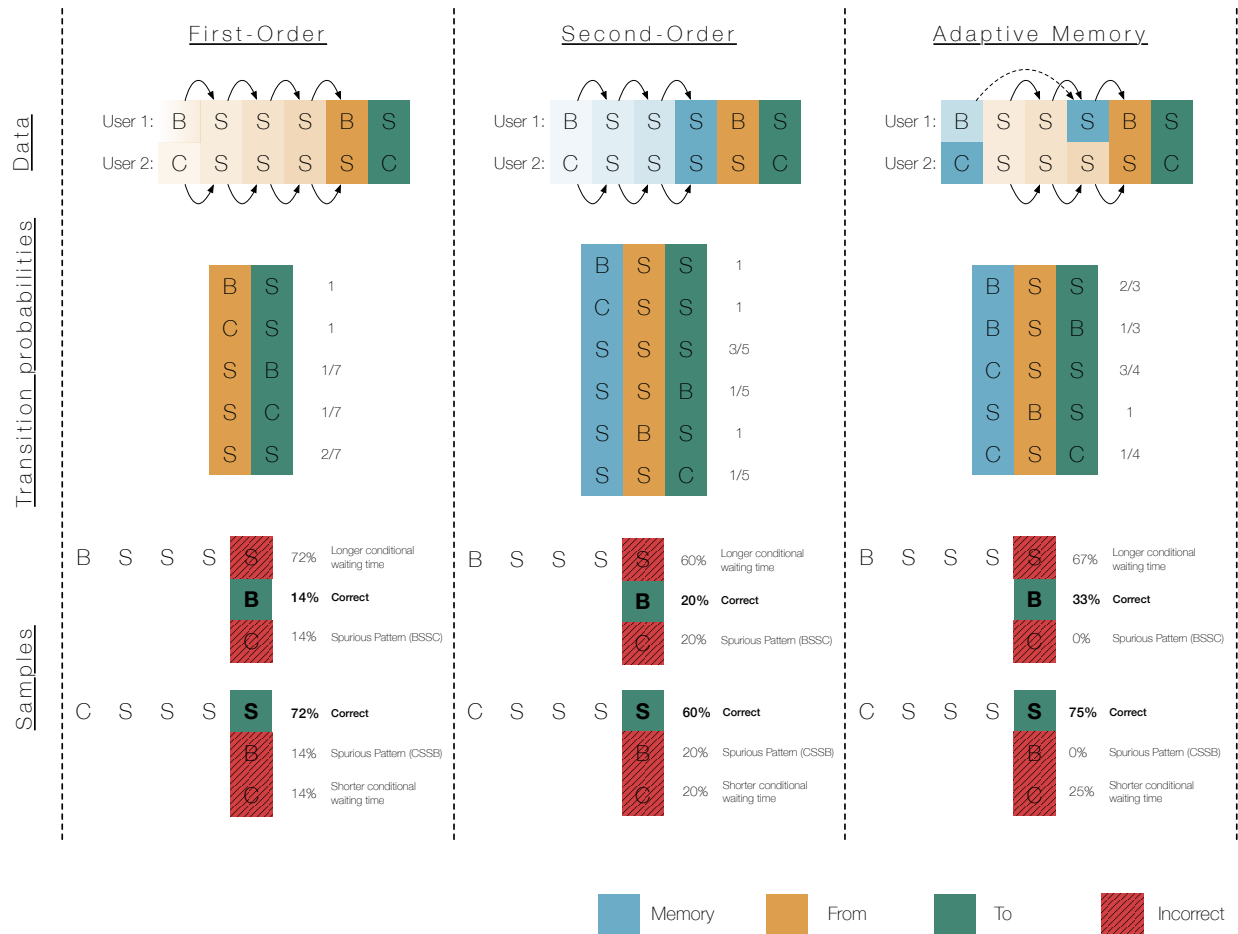


FIG. 3. **Predicting individual mobility.** Using the sequence of calls made by two different users (1 and 2) – starting from two different locations (B and C) and visiting a new location S – we build first-order and second-order Markov models, as well as the adaptive memory one. We use each mobility model to generate the possible mobility sequences. Given that there are two empirical starting points, we originated the sampled sequences in B and C, respectively. In the figure, for each sample, we report the fraction of times it is reproducing observation (“Correct”), it is a non-observed mobility pattern (“Spurious Pattern”) and it is underestimating or overestimating waiting times (“Longer/Shorter Conditional Waiting Time”).

177 processes such as epidemics spreading.

178

C. Overview of the dataset

179 In the next section, we will quantify the impact of adaptive memory on human mobility mod-
 180 eling by using data sets provided by the Data for Development Challenge 2014 [27] and some
 181 supplementary data sets provided by partners of the challenge. Mobile phone data consist of com-
 182 munications among 1666 towers distributed across Senegal. We exploit this information to map

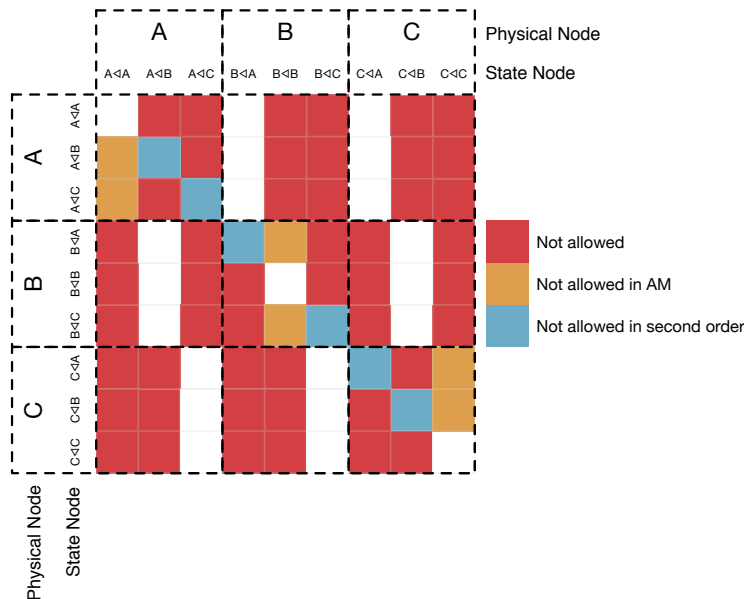


FIG. 4. **Mobility Matrix** Second-order transition matrix for three physical nodes A, B and C. The state nodes are represented with the notation $x \prec y$ meaning that walkers in this node have traveled from node y to node x . The cells in red are not used by either second-order markovian model or adaptive memory model. The cells in bluish are used only in adaptive memory model, while, the cells in orange are used only in the second-order markovian model. The cells in white are used by both models.

183 communication patterns between different areas of the country (i.e. the arrondissements). Another
 184 subset consists of 560 millions call records of about 150,000 users along one year at at the spatial
 185 resolution of arrondissements. We use this information to map individuals' movements among
 186 different arrondissements. Demographics information has been obtained from the Senegal data
 187 portal [28], an official resource. It is worth noting that information has been manually checked
 188 against inconsistencies and data about population for the arrondissements of Bambilor, Thies Sud,
 189 Thies Nord, Ndiob and Ngothie were not available. We reconstructed the missing information by
 190 combining mobile phone activity and available demographics data (Fig. 5). Such arrondissements
 191 did not exist at the time when the population census was obtained, because they were part of
 192 larger administrative areas. Information is available for older arrondissements, therefore we devise
 193 a procedure to infer the population in the new areas by using phone calls as a proxy to population
 194 density.

195 We have used the data to also infer more realistic contact rates to be used in viral spreading
 196 simulations. The contacts among individuals are generally quite difficult to track at country level.
 197 Their rate varies depending on several social and demographical factors such as age, gender, lo-

198 cation, urban development, *etc.* [29, 30]. Nevertheless, there are evidences from European and
 199 African countries that, on average, the number of daily physical contacts among individuals range
 200 from 11 to 22 [29, 30]. There are no available data about contact rate in each arrondissement
 201 of Senegal, therefore we need to infer this information from available sources. We first estimate
 202 the population density for each region, an administrative level coarser than arrondissement, using
 203 available data about number of inhabitants and area. As a plausible range of contact rates, we
 204 consider 10 and 25. Under the assumption that the contact rate is proportional to the population
 205 density, we assign a value to each region that ranges between 10 and 25, with extremal values
 206 assigned to the regions with lowest and highest population density, respectively. Therefore, we
 207 assign the same contact rate to all arrondissements pertaining to the same region. We obtain a
 208 contact rate between 10 and 11 for all regions, except Dakar which has the highest population
 209 density.

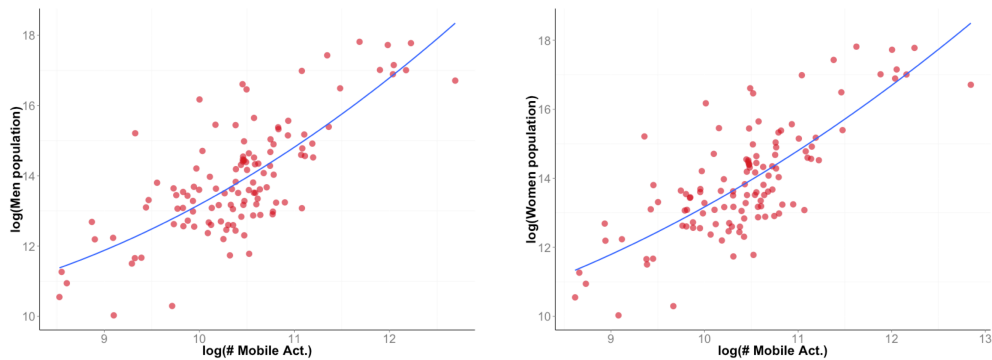


FIG. 5. **Inferring men and women populations.** Second-order polynomial model (solid line) fitting the log-log relationships between the observed mobile phone data and demographics data (points). Men (A) and women (B) population were fitted separately, thanks to data availability, and have been used to infer the populations in the arrondissements of Bambilor, Thies Sud, Thies Nord, Ndiob and Ngothie.

III. RESULTS

A. Understanding human mobility flow

212 We show in Fig.6 the significant differences in modeling the mobility flow using first-order
 213 (FO), second-order (SO) and adaptive memory (AM) models. Markovian models provide very
 214 similar transition patterns, whereas adaptive memory provides very different results. The adaptive
 215 memory model exhibits significantly less returning transitions than Markovian models, but – on
 216 average – with much higher probability of observing them. In fact, 47.4% of patterns captured

217 by the first-order approach and 43.4% captured using second-order are spurious because they are
 218 not observed in reality. Remarkably, the probability that an individual comes back to her origin is
 219 on average six times higher using adaptive memory models than using first-order, and five times
 220 higher using second-order. In the Supplementary Material, we show the result of the same analysis
 221 for the gravity model [31, 32] and the more recent radiation model [4, 33], two widely adopted
 222 approaches to model human mobility.

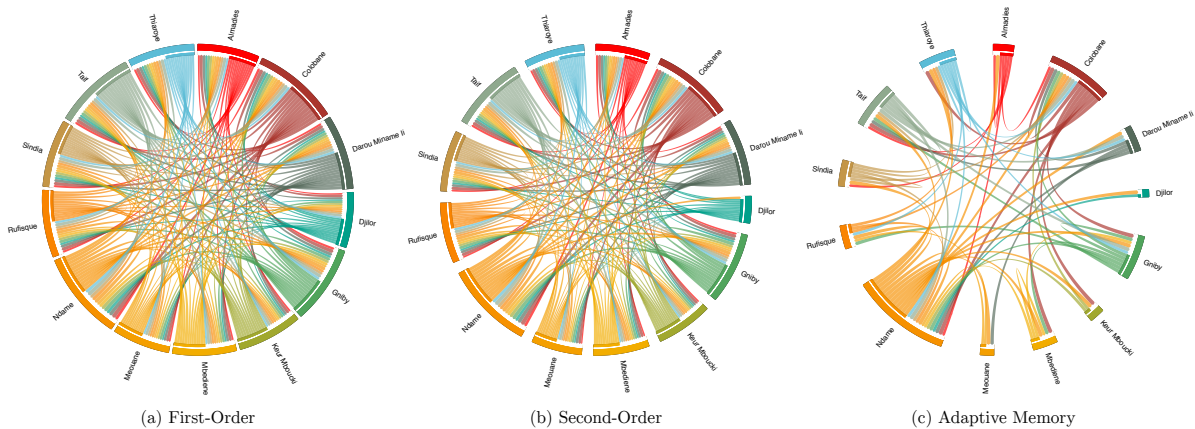


FIG. 6. **Mobility flow among a sub-set of Senegal’s arrondissements.** For simplicity, we illustrate the effects of each model by considering a subset of 13 arrondissements and patterns that goes through one specific arrondissement (Kael, in this example) after departing from their origin and before reaching their destination. The figure shows the mobility modeled by means of first-order (A), second-order (B) and adaptive 2-memory (C), putting in evidence the different mobility patterns between Markovian models and adaptive memory. For instance, the adaptive memory module captures returning patterns (i.e. movements like $X \rightarrow \text{Kael} \rightarrow X$) better than the first-order model. See Supplementary Material for results obtained from gravity and radiation models.

223 To compare the accuracy of both models against the mobility behavior observed in data, we
 224 use the coverage, defined as the fraction of nodes visited by an individual within a given amount
 225 of time. We calculate the coverage for each individual in the data, over a period of one months,
 226 and then we average over all arrondissements to obtain a measure at country level. For the same
 227 period of time, we generate three transition matrices \mathbf{F} , \mathbf{H} and \mathbf{A} encoding the mobility dynamics
 228 for first-order, second-order and adaptive memory models, respectively. To better replicate the
 229 calling behavior of the individuals in the data set, we extract information about the distribution of
 230 time between calls and we use this information in our simulations (see Supplementary Material).

231 In Fig. 7A and B we show that people diffuse in the country too fast using Markovian models,

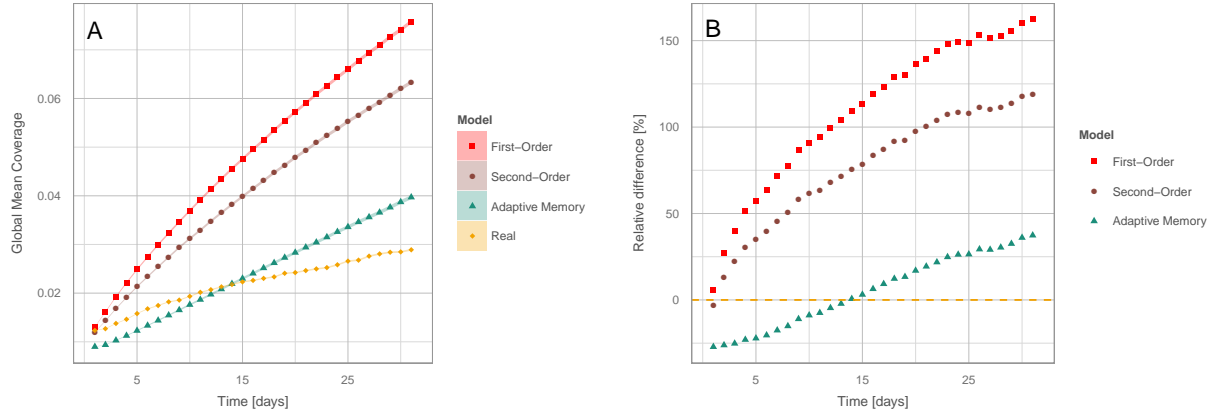


FIG. 7. **Observed human mobility and theoretical predictions.** (A) Temporal evolution of the global mean coverage calculated from real data and from simulations using first-order (FO), second-order (SO) and adaptive memory (AM) models. (B) Relative difference between the coverage observed in real human mobility and the one obtained from simulations. See Supplementary Material for results obtained from gravity and radiation models.

232 whereas significantly slower diffusion is found with adaptive memory, in agreement with empirical
 233 observation. In the Supplementary Material, we show the result of the same analysis for both the
 234 gravity and the radiation models. We observe that the gravity model is not suitable to reproduce the
 235 observation, whereas the radiation model provides results comparable with the adaptive memory
 236 model proposed in this study.

237 These results have deep implications, for instance, in short-term or long-term predictions of
 238 epidemic spreading or national infrastructure planning.

239 B. Impact of human mobility models on the spreading of epidemics

240 Here, we focus on epidemic spreading. How infectious individuals move among different locations
 241 has a strong influence in how diseases diffuse in a population. We considered each arrondissement as
 242 a meta-population where any individual can interact with a limited number of other individuals.
 243 We use a SEIR compartmental model [34] to characterize the epidemics evolution within each
 244 arrondissement and mobility models to simulate people traveling in the country.

245 The discrete time step of the following models is $\Delta t \approx 1$ hour, approximately the observed
 246 median between two successive calls from the same individual. The parameters are demographical
 247 and epidemiological. Demographics parameters include the birth $B = \tilde{B}\Delta t$ and death $\delta = \tilde{\delta}\Delta t$
 248 probability, whereas epidemiological parameters correspond to the latent period τ_E of the infection,

249 from which the probability $\epsilon = \Delta t / \tau_E$ to pass to the infectious state is calculated, and the infectious
 250 period τ_I , from which the probability $\gamma = \Delta t / \tau_I$ to recover from or die because of the infection is
 251 calculated. The last parameter is the effective transmission probability

$$\beta_i(t) = 1 - \left(1 - \tilde{\beta} \Delta t \frac{I_i(t)}{N_i(t)} \right)^{c_i \Delta t}, \quad (4)$$

252 an arrondissement-dependent parameter that depends on the average number of contacts per unit
 253 of time c_i experienced by an individual in node i , the fraction of infected individuals in that
 254 node and the transmission risk $\tilde{\beta} \Delta t$ in case of contact with an infectious individual. In fact, the
 255 definition of $\beta_i(t)$ induces a type-II reaction-diffusion dynamics [9] accounting for the fact that each
 256 individual does not interact with *all* the other individuals in the meta-population, but only with
 257 a limited sample. If the number of infected agents is small (i.e. $I_i(t) \approx 0$) the Taylor expansion
 258 of $\beta_i(t)$ truncated at the first order gives the classical factor $\tilde{\beta} \Delta t c_i \Delta t \frac{I_i(t)}{N_i(t)}$ [34]. It follows that
 259 the equations describing the average spreading of a disease according to a SEIR model coupled to
 260 first-order mobility are given by

$$\begin{aligned} S_i(t+1) &= \sum_{j=1}^n F_{ji} [(1 - \delta - \beta_j(t)) S_j(t) + B N_j(t)] \\ E_i(t+1) &= \sum_{j=1}^n F_{ji} [(1 - \epsilon - \delta) E_j(t) + \beta_j(t) S_j(t)] \\ I_i(t+1) &= \sum_{j=1}^n F_{ji} [(1 - \gamma - \delta) I_j(t) + \epsilon E_j(t)] \\ R_i(t+1) &= \sum_{j=1}^n F_{ji} [(1 - \delta) R_j(t) + \gamma I_j(t)] \end{aligned} \quad (5)$$

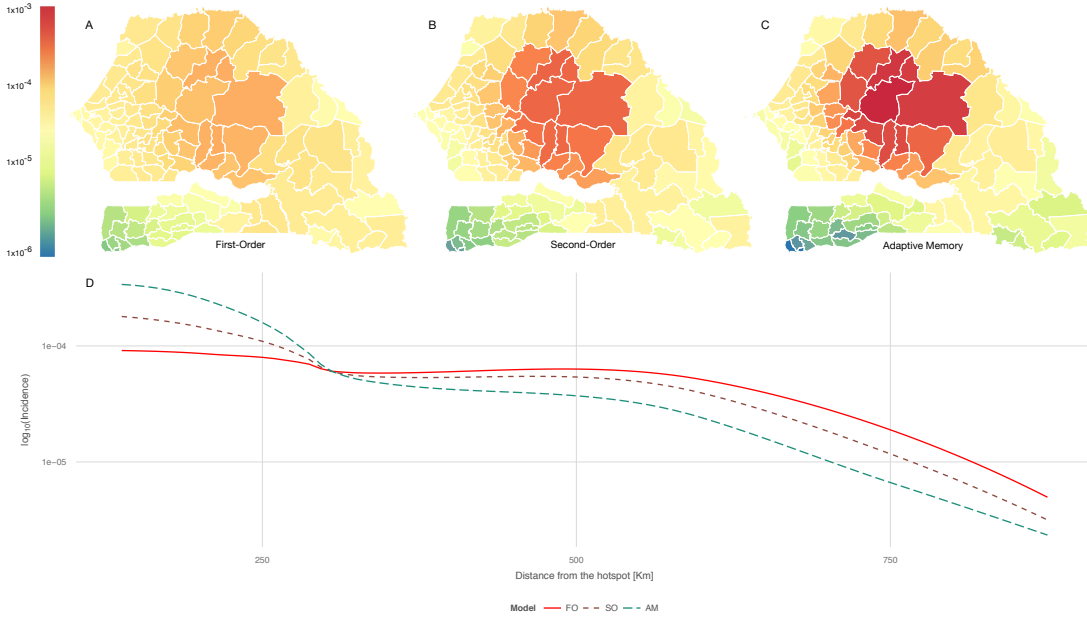


FIG. 8. Spreading of an influenza-like outbreak in Senegal. We show the incidence of an influenza-like virus over Senegal arrondissements a week after the infection onset, using first-order (A), second-order (B) and adaptive 2-memory (C) mobility models. The infection started in Barkedji (center of Senegal), where three individuals are initially infected. A SEIR compartmental dynamics with parameters $\beta = 0.05$, $\epsilon = 0.2$, $\gamma = 0.5$ is used to simulate the spreading of the disease within each arrondissement. We found that the number of arrondissements with infected individuals is higher using Markovian dynamics. Conversely, the adaptive memory favors a higher concentration of infected individuals in the arrondissements around the initial location of the infection. In fact, the location of the onset of the epidemic can be better identified using adaptive memory rather than Markovian models. (D) Relation between the incidence in a region and the distance from the hotspot of the infection using the three models. Adaptive memory models spread the incidence on regions closer to the hotspot and this effect is even more evident when higher memory is used.

261 whereas the coupling to the second-order model is given by

$$\begin{aligned}
\tilde{S}_\alpha(t+1) &= \sum_{\psi=1}^{n^2} H_{\psi\alpha} \left[(1 - \delta - \tilde{\beta}_\psi^{(\alpha)}(t)) \tilde{S}_\psi(t) + B \tilde{N}_\psi(t) \right] \\
\tilde{E}_\alpha(t+1) &= \sum_{\psi=1}^{n^2} H_{\psi\alpha} \left[(1 - \epsilon - \delta) \tilde{E}_\psi(t) + \tilde{\beta}_\psi^{(\alpha)}(t) \tilde{S}_\psi(t) \right] \\
\tilde{I}_\alpha(t+1) &= \sum_{\psi=1}^{n^2} H_{\psi\alpha} \left[(1 - \gamma - \delta) \tilde{I}_\psi(t) + \epsilon \tilde{E}_\psi(t) \right] \\
\tilde{R}_\alpha(t+1) &= \sum_{\psi=1}^{n^2} H_{\psi\alpha} \left[(1 - \delta) \tilde{R}_\psi(t) + \gamma \tilde{I}_\psi(t) \right] \\
\tilde{\beta}_\psi^{(\alpha)}(t) &= 1 - \left(1 - \tilde{\beta} \Delta t \frac{\sum_{\rho=\lfloor \frac{\alpha}{n} \rfloor n+1}^{\lfloor \frac{\alpha}{n} \rfloor n+n} \tilde{I}_\rho(t)}{\sum_{\rho=\lfloor \frac{\alpha}{n} \rfloor n+1}^{\lfloor \frac{\alpha}{n} \rfloor n+n} \tilde{N}_\rho(t)} \right)^{c_i \Delta t} \tag{6}
\end{aligned}$$

262 where $N(t) = \sum_{\psi=1}^{n^\tau} \tilde{N}_\psi(t)$ is the total population in the country at time t , $\lfloor \cdot \rfloor$ indicates the floor
263 function and is used to identify the sub-set of state-nodes corresponding to the same physical node
264 the population \tilde{S}_α belongs to. The equations for the adaptive memory model are the same, except
265 that the transition matrix \mathbf{A} is used instead of \mathbf{H} .

266 We initiate the simulation by infecting five individuals in Barkedji, at the center of Senegal.
267 The differences between the diffusion of the infective process using each mobility model are quite
268 visible in Fig. 8. The spreading is faster for Markovian models, with some arrondissement populated
269 by more infected individuals than adaptive memory. The incidence, i.e. the fraction of infected
270 individuals in an arrondissement, follows different spatial patterns in the three models (see Fig. 8A–
271 C), with a higher incidence observed in the origin of the infection that decreases as we move far from
272 there. This effect is significantly stronger using adaptive memory because it tends to concentrate
273 more infectious individuals close to the origin (see Fig. 8D).

274

DISCUSSION

275 Modeling how people move among different locations is crucial for several applications. Given
276 the scarcity of information about individuals' movements, often human mobility proxies such as
277 call detail records, GPS, *etc*, are used instead. Here, we have shown that dynamical models
278 built from human mobility proxies can be significantly wrong, underestimating (or overestimating)
279 real mobility patterns or predicting spurious movements that are not observed in reality. We

280 have proposed a general solution to this issue, by introducing an adaptive memory modeling of
281 human mobility that better captures observed human dynamics and dramatically reduces spurious
282 patterns with respect to memoryless or higher-order Markovian models. However, it is worth
283 remarking that this approach, as all other methods in the literature, is based on the assumption
284 that an individual makes a call in each place he or she visits. In fact, this is not always true and
285 care must be taken when interpreting the results. Fortunately, an appropriate choice of the spatial
286 granularity, for instance at administrative levels corresponding to cities or larger areas, reduces
287 this unavoidable effect. We have validated our model on a data set consisting of 560 millions of call
288 detail records from Senegal. We have found that individuals tend to diffuse faster with standard
289 mobility models than what observed in reality, whereas the adaptive memory approach reconciles
290 empirical observations and theoretical expectations. Our findings have, for instance, a deep impact
291 on predicting how diseases spread in a country. While standard approaches tending to overestimate
292 the geographical incidence of the infection, the more realistic modeling obtained by means of
293 adaptive memory can improve the inference of the hotspot of the infection, helping to design
294 better countermeasures, e.g. more effective quarantine zones, improved resources deployment or
295 targeted information campaigns.

296 **COMPETING INTERESTS**

297 The authors declare that they have no competing interests.

298 **DATA ACCESSIBILITY**

299 The data used in this manuscript were made publicly available during the D4D Senegal Chal-
300 lenge organized by Orange. More information about data can be found here: [http://www.d4d.
301 orange.com/en/presentation/data](http://www.d4d.orange.com/en/presentation/data)

302 **AUTHOR'S CONTRIBUTIONS**

303 JTM and MDD contributed equally to this work. JTM and MDD developed the theoretical
304 model and carried out the statistical analyses; MDD and AA conceived of the study, designed the
305 study and coordinated the study. All authors wrote the manuscript and gave final approval for
306 publication.

FUNDING

307

308 M.D.D. acknowledges financial support from the Spanish program Juan de la Cierva (IJCI-
 309 2014-20225). JTM was supported by Generalitat de Catalunya (FI-DGR 2015). A.A. acknowl-
 310 edges financial support from ICREA Academia and James S. McDonnell Foundation and Spanish
 311 MINECO FIS2015-71582.

-
- 312 [1] Gonzalez MC, Hidalgo CA, Barabasi AL. Understanding individual human mobility patterns. *Nature*.
 313 2008;453(7196):779–782.
- 314 [2] Balcan D, Colizza V, Gonçalves B, Hu H, Ramasco JJ, Vespignani A. Multiscale mobility networks
 315 and the spatial spreading of infectious diseases. *PNAS*. 2009;106(51):21484–21489.
- 316 [3] Song C, Qu Z, Blumm N, Barabási AL. Limits of predictability in human mobility. *Science*.
 317 2010;327(5968):1018–1021.
- 318 [4] Simini F, González MC, Maritan A, Barabási AL. A universal model for mobility and migration
 319 patterns. *Nature*. 2012;484(7392):96–100.
- 320 [5] Lima A, Stanojevic R, Papagiannaki D, Rodriguez P, González MC. Understanding individual routing
 321 behaviour. *Journal of The Royal Society Interface*. 2016;13(116).
- 322 [6] Balcan D, Vespignani A. Phase transitions in contagion processes mediated by recurrent mobility
 323 patterns. *Nature Phys*. 2011;7(7):581–586.
- 324 [7] Rosvall M, Esquivel AV, Lancichinetti A, West JD, Lambiotte R. Memory in network flows and its
 325 effects on spreading dynamics and community detection. *Nature Communications*. 2014;5:4630.
- 326 [8] Ferguson NM, Cummings DA, Cauchemez S, Fraser C, Riley S, Meeyai A, et al. Strategies for containing
 327 an emerging influenza pandemic in Southeast Asia. *Nature*. 2005;437(7056):209–214.
- 328 [9] Colizza V, Pastor-Satorras R, Vespignani A. Reaction–diffusion processes and metapopulation models
 329 in heterogeneous networks. *Nature Phys*. 2007;3(4):276–282.
- 330 [10] Wesolowski A, Eagle N, Tatem AJ, Smith DL, Noor AM, Snow RW, et al. Quantifying the impact of
 331 human mobility on malaria. *Science*. 2012;338(6104):267–270.
- 332 [11] Eagle N, Pentland A. Reality mining: sensing complex social systems. *Personal and ubiquitous com-
 333 puting*. 2006;10(4):255–268.
- 334 [12] Eagle N, Pentland AS, Lazer D. Inferring friendship network structure by using mobile phone data.
 335 *PNAS*. 2009;106(36):15274–15278.
- 336 [13] Deville P, Linard C, Martin S, Gilbert M, Stevens FR, Gaughan AE, et al. Dynamic population
 337 mapping using mobile phone data. *PNAS*. 2014;111(45):15888–15893.
- 338 [14] Amini A, Kung K, Kang C, Sobolevsky S, Ratti C. The impact of social segregation on human mobility
 339 in developing and industrialized regions. *EPJ Data Science*. 2014;3(1):6.

- 340 [15] Tizzoni M, Bajardi P, Decuyper A, Kon Kam King G, Schneider C, et al . On the Use of Human
341 Mobility Proxies for Modeling Epidemics. *PLoS Comput Biol.* 2014;10(7):e1003716.
- 342 [16] Wesolowski A, Buckee C, Bengtsson L, Wetter E, Lu X, Tatem A. Commentary: Containing the Ebola
343 outbreak—the potential and challenge of mobile network data. *PLoS Curr Outbr.* 2014;.
- 344 [17] Calabrese F, Ferrari L, Blondel VD. Urban Sensing Using Mobile Phone Network Data: A Survey of
345 Research. *ACM Computing Surveys (CSUR).* 2014;47(2):25.
- 346 [18] Blondel VD, Decuyper A, Krings G. A survey of results on mobile phone datasets analysis. To appear
347 in *EPJ Data Science.* 2015;.
- 348 [19] Wesolowski A, Eagle N, Noor AM, Snow RW, Buckee CO. Heterogeneous mobile phone ownership and
349 usage patterns in Kenya. *PLoS ONE.* 2012;7(4):e35319.
- 350 [20] Eagle N, de Montjoye Y, Bettencourt LM. Community computing: Comparisons between rural and
351 urban societies using mobile phone data. In: *Computational Science and Engineering, 2009. CSE'09.*
352 *International Conference on.* vol. 4. IEEE; 2009. p. 144–150.
- 353 [21] Dobra A, Williams NE, Eagle N. Spatiotemporal Detection of Unusual Human Population Behavior
354 Using Mobile Phone Data. *PLoS ONE.* 2014;p. DOI:10.1371/journal.pone.0120449.
- 355 [22] Lima A, De Domenico M, Pejovic V, Musolesi M. Disease Containment Strategies based on Mobility
356 and Information Dissemination. *Scientific Reports.* 2015;5:10650.
- 357 [23] Colizza V, Vespignani A. Epidemic modeling in metapopulation systems with heterogeneous coupling
358 pattern: Theory and simulations. *J Theor Bio.* 2008;251(3):450–467.
- 359 [24] Tatem AJ, Adamo S, Bharti N, Burgert CR, Castro M, Dorelien A, et al. Mapping populations at
360 risk: improving spatial demographic data for infectious disease modeling and metric derivation. *Popul*
361 *Health Metr.* 2012;10(8).
- 362 [25] Pandey A, Atkins KE, Medlock J, Wenzel N, Townsend JP, Childs JE, et al. Strategies for containing
363 Ebola in west Africa. *Science.* 2014;346(6212):991–995.
- 364 [26] Wesolowski A, Buckee CO, Pindolia DK, Eagle N, Smith DL, Garcia AJ, et al. The use of cen-
365 sus migration data to approximate human movement patterns across temporal scales. *PLoS ONE.*
366 2013;8(1):e52971.
- 367 [27] de Montjoye YA, Smoreda Z, Trinquart R, Ziemlicki C, Blondel VD. D4D-Senegal: The Second Mobile
368 Phone Data for Development Challenge. arXiv:14074885. 2014;.
- 369 [28] ;. <http://donnees.ansd.sn/en/>.
- 370 [29] Rohani P, Zhong X, King AA. Contact network structure explains the changing epidemiology of
371 pertussis. *Science.* 2010;330(6006):982–985.
- 372 [30] Kiti MC, Kinyanjui TM, Koech DC, Munywoki PK, Medley GF, Nokes DJ. Quantifying age-related
373 rates of social contact using diaries in a rural coastal population of Kenya. *PloS one.* 2014;9(8):e104786.
- 374 [31] Zipf GK. The P 1 P 2/D hypothesis: on the intercity movement of persons. *American sociological*
375 *review.* 1946;11(6):677–686.
- 376 [32] Barthélemy M. Spatial networks. *Physics Reports.* 2011;499(1):1–101.

- 377 [33] Ren Y, Ercsey-Ravasz M, Wang P, González M, Toroczkai Z. Predicting commuter flows in spatial
378 networks using a radiation model based on temporal ranges. *Nature communications*. 2013;5:5347–5347.
- 379 [34] Keeling MJ, Rohani P. *Modeling infectious diseases in humans and animals*. Princeton University
380 Press; 2008.

